1962

Performance of a phase modulation system using pseudorandom coding

Meredith Sherman Ulstad
Iowa State University

PERFORMANCE OF A PHASE MODULATION SYSTEM USING PSEUDORANDOM CODING

by

Meredith Sherman Ulstad

A Dissertation Submitted to the
Graduate Faculty in Partial Fulfillment of
The Requirements for the Degree of
DOCTOR OF PHILOSOPHY

Major Subject: Electrical Engineering

Approved:

Signature was redacted for privacy.

In Charge of Major Work

Signature was redacted for privacy.

Head of Major Department

Signature was redacted for privacy.

Dean of ~~Graduate~~ College

Iowa State University
Of Science and Technology
Ames, Iowa

1962

TABLE OF CONTENTS

I. INTRODUCTION

As a result of theoretical work published by Shannon (1) in 1948 and continued by numerous other workers, it is now possible to quantitatively determine the performance of communication systems. Shannon established a formula which sets a theoretical "standard of excellence" against which systems with widely different parameters can be compared. This formula is shown in Equation 1.

$$C_{SH} = W \log_2 (1 + \beta^2) \qquad 1$$

Shannon proved that if sufficiently elaborate coding methods are used, C_{SH} bits of information per second may be sent through a channel having W cycles per second bandwidth and an average signal-to-noise power ratio β^2 with arbitrarily low rate of error. This assumes that the noise power is additive, gaussian, and white over the entire bandwidth W. Figure 1 shows the system model upon which this formula is based.

In this paper, a communication system similar to that shown in Figure 1 will be studied. Several additional restrictions are, however, placed upon the encoder and decoder. The output power of the encoder must be substantially confined to a narrow band of frequencies, W, centered at ω_o radians per second. Furthermore, it is required that information shall be conveyed only in the phase of this narrowband signal. The work proceeds in two steps, basically. First, a formula analogous to Equation 1 is derived for the more restricted channel hereafter called the PM or phase modulated channel. Second, a communication

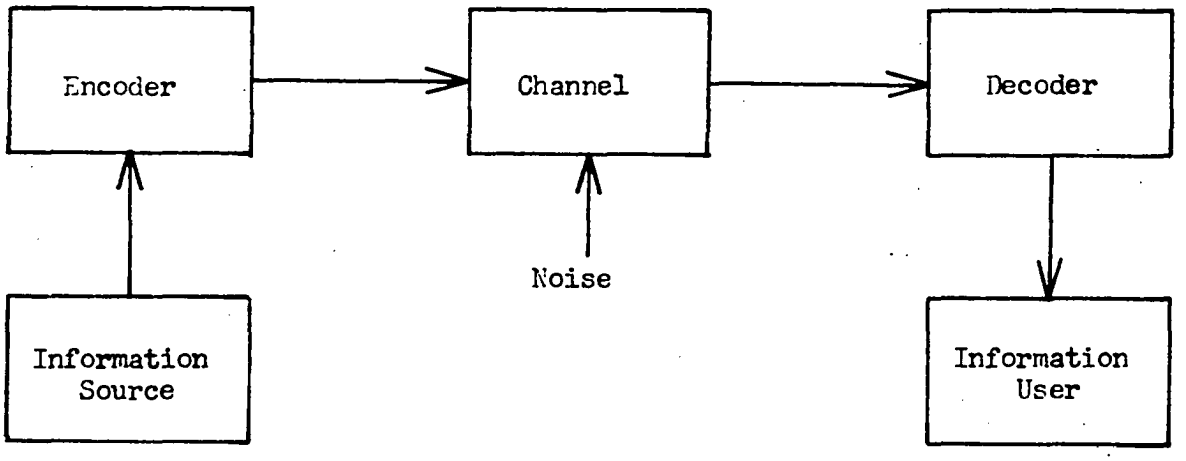

Figure 1. Block diagram of communication system

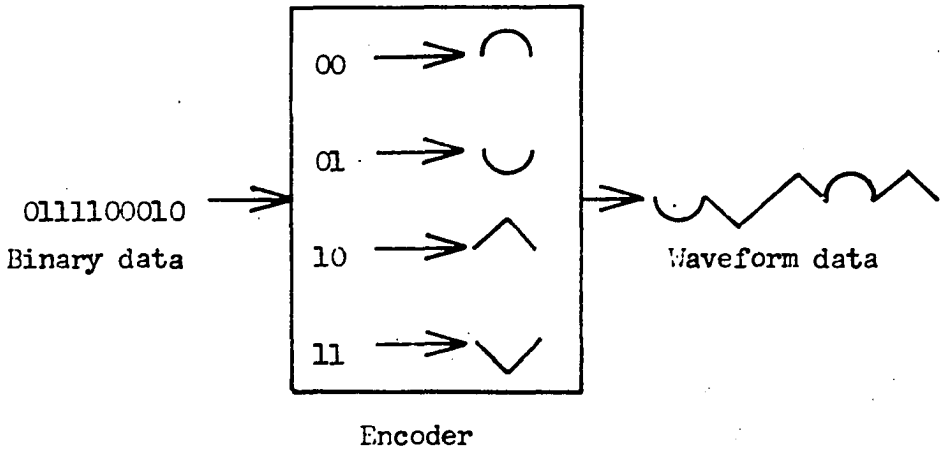

Figure 2. Example of a Woodward encoder for M = 4

system has been proposed for which the performance will be computed.

The proposed communication system is known a priori to be suboptimum in that a superior system can be readily suggested. However, the optimum system is very much more difficult to actually implement. In the proposed system each subsystem function, defined only mathematically in this paper, can be constructed without great difficulty.

Consider an encoder capable of sequentially generating waveforms $x_i(t)$, $x_j(t)$, $\cdots\cdots x_p(t)\cdots$ in response to properly processed input information. All of these waveforms (of which $M > 1$ are available) are assumed to be of equal time duration and individually distinct. An example of such an encoder using $M = 4$ is shown in Figure 2. Woodward (2) has proven that if time stationary gaussian noise is added to the output of this encoder, no decoder can do better than to process the noisy signal by cross-correlation. This means that all of the M possible encoder output waveforms must be stored by the decoder and compared with the noisy received signals. The locally available signal having the greatest cross-correlation is then assumed to have been the one actually sent by the encoder. Using this fact, Fano (3) proposed his "Idealized Communication System" shown in Figure 3. This system uses the basic ideas advanced by Woodward (2).

The proposed communication system studied in this paper strongly resembles the one proposed by Fano (3). However, great practical difficulties arise when the decoder is located far from or moving with respect to the encoder. The principal difficulties arise in attempting to determine the precise time of arrival and in generating of high frequency waveforms

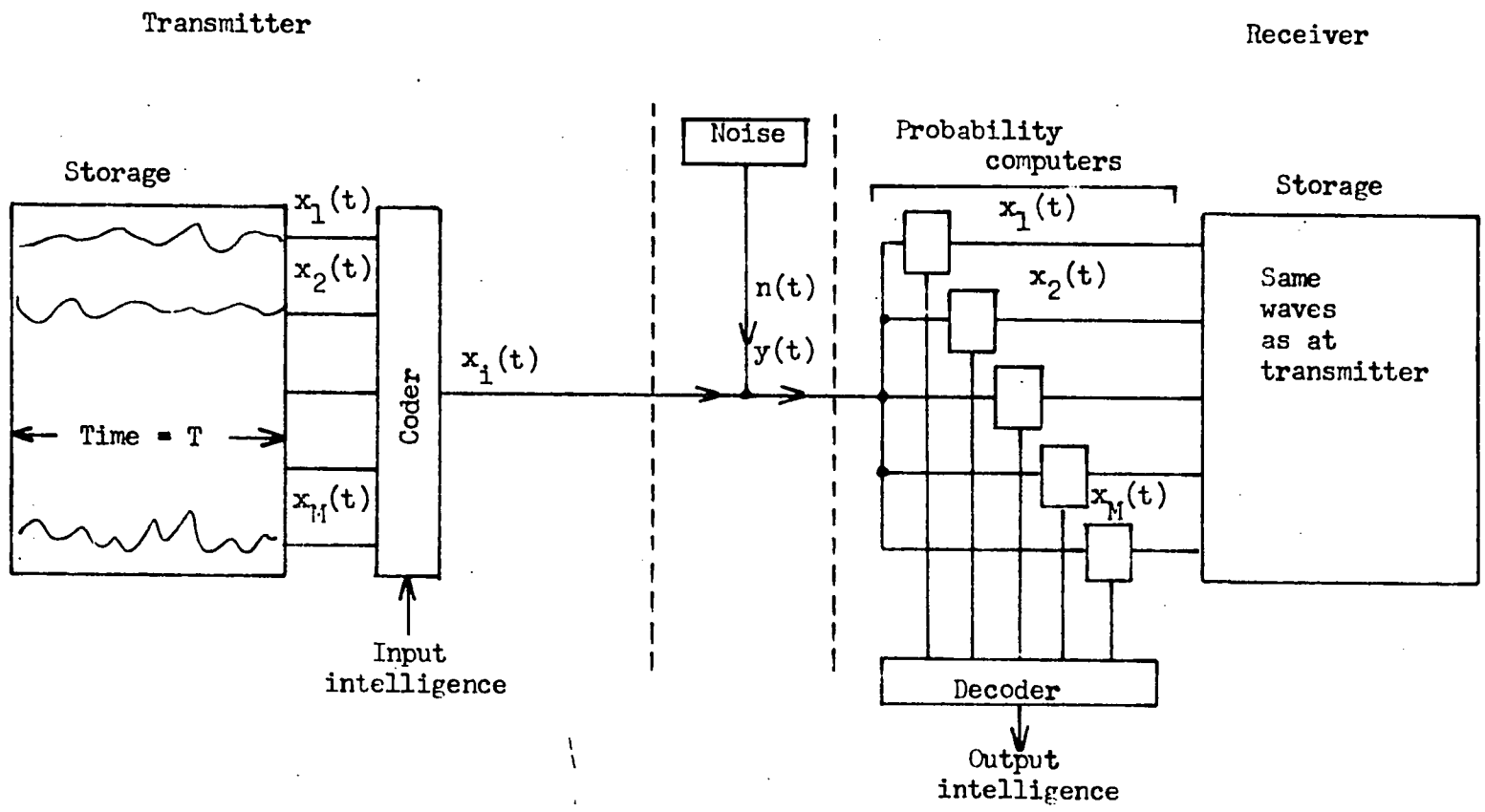

Figure 3. Fano's "Idealized Communication System"

at the decoder. The communication system studied in this paper attempts to circumvent these problems while maintaining good performance.

Quite recently a practical communication system similar to the one suggested by Fano (3) was described by Sanders (4). This system employed digital phase modulation and used a phase locked detection system. The spectrum generated by such an encoder is not well defined or as narrow as is possible. It was, nevertheless, well suited to the missile telemetry application for which it was intended. The detection system, furthermore, becomes useless for values of β^2 in the vicinity of unity. The proposed system, on the other hand, has a narrow, well defined spectrum and has no basic detector threshold problem.

In order to prove that communication systems carrying information only in the phase of narrowband signals can perform at nearly the Shannon (1) rate, it is now necessary to determine C_{PM}/C_{SH}. This ratio represents the fractional part of the more general Shannon channel capacity which is obtainable with phase modulation.

II. CHANNEL CAPACITY FOR PHASE MODULATION

A. Maximum Encoder Entropy

In order to derive the expression for C_{PM}, steps analogous to those originally used by Shannon (1) are outlined below.

1. The entropy, $H(\lambda)$ of $p[\lambda]$ must be calculated. The parameter λ will designate encoder output phase hereafter.

$$H(\lambda) = - \int_{-\infty}^{\infty} p[\lambda] \log_e p[\lambda] \, d\lambda \qquad 2$$

2. The conditional entropy of $p[\lambda|\varphi]$ must be calculated. φ represents the input signal phase at the decoder.

$$H(\lambda \varphi) = - \int_{-\infty}^{\infty} \int_{-\infty}^{\infty} p[\varphi]p[\lambda|\varphi] \log_e p[\lambda|\varphi] \, d\lambda d\varphi \qquad 3$$

3. Determine the channel capacity C_{PM}.

$$C_{PM} = H(\lambda) - H(\lambda|\varphi) \qquad 4$$

The quantity $H(\lambda|\varphi)$ is a measure of the uncertainty of λ given φ. $H(\lambda|\varphi)$ is completely determined by β^2. Therefore, to obtain channel capacity, $H(\lambda)$ should be maximized subject to the constraint imposed by Equation 5.

$$\int_{-\infty}^{\infty} p[\lambda] d\lambda = 1 \qquad 5$$

Investigation into C_{PM} was made by Blachman (5). His work resulted in asymptotic values for very large and very small values of β^2. In this study, a digital computer was used to verify Blachman's asymptotes and to compute intermediate values.

$H(\lambda)$, as given by Equation 2 and constrained by Equation 5, may be

maximized using calculus of variations. To do this, solve Equation 6 for p and substitute the resulting expression for p into Equation 5. The range of the variable λ may be restricted as in Equation 8 for reasons shown in Appendix B.

$$-\frac{\partial(p \log_e p)}{\partial p} + m \frac{\partial p}{\partial p} = 0 \qquad 6$$

$$1 + \log_e p = m \qquad 7$$

Therefore $p[\lambda]$ is a constant. Using the constraint imposed by Equation 5 leads to

$$p[\lambda] = \frac{1}{2\pi} = p_o[\lambda]. \qquad 8$$

$$-\pi \leq \lambda \leq \pi$$

The maximum value of $H(\lambda)$ is therefore

$$H(\lambda) = \log_e 2\pi. \qquad 9$$

By representing the signal function, $s_2(t)$, and the random noise function, $\propto(t)$, each as a long sequence of sampling functions (per Appendix B) the average information per sample point can be determined using Equation 4. In order to do this, however, it is first necessary to obtain $H(\lambda|\varphi)$.

B. Channel Capacity

The signal function, $s_2(t)$, will be considered to consist of a superposition of sampling functions with sample points separated by $\mu = \frac{1}{W}$ seconds. This is expressed mathematically by

$$s_2(t) = \sum_{k=1}^{Q} A \frac{\sin \frac{\pi}{\mu}(t - k\mu)}{\frac{\pi}{\mu}(t - k\mu)} \cos(\omega_o t + \lambda_k) . \qquad 10$$

Q is taken to be a large integer in Equation 10.

In the same way, the representative noise function $\alpha(t)$ can be represented as

$$\alpha(t) = \sum_{k=1}^{Q} N_k \frac{\sin \frac{\pi}{\mu}(t - k\mu)}{\frac{\pi}{\mu}(t - k\mu)} \cos(\omega_o t + \rho_k) . \qquad 11$$

Bennett (6) shows that the set of amplitude parameters, N_k, are statistically independent and their individual probability density function are Rayleigh distributed. The mean square value of the random variable N_k is $2\sigma^2$. The set of parameters ρ_k are also independent. The probability density function for the random variable ρ_k is

$$p_o[\rho_k] = \frac{1}{2\pi} , \quad -\pi \leq \rho_k \leq \pi \qquad 12$$
$$= 0, \quad |\rho_k| > \pi .$$

The envelope function of Equation 10 varies slowly with time compared to the cos $\omega_o t$ term. Thus, very near to any particular sample point k the function $s_2(t)$ is essentially sinusoidal with amplitude A and phase λ_k. In like manner the noise function is approximately sinusoidal with random phase ρ_k and amplitude N_k. Through the use of Appendix A the probability density function for λ given φ is written as

$$p_1[\lambda|\varphi] = \frac{\exp(-\beta^2)}{[2\pi]} + \frac{\beta}{\sqrt{\pi}} \cos(\lambda - \varphi) \exp[-\beta^2 \sin^2(\lambda - \varphi)] \frac{1}{\sqrt{2\pi}} \int_{-\infty}^{\sqrt{2}\beta\cos(\lambda-\varphi)} \exp(-\frac{t^2}{2})\, dt \qquad 13$$

$$-\pi \leq \lambda \leq \pi.$$

A, β, and σ are related by

$$\beta^2 = \frac{A^2}{2\sigma^2}. \qquad 14$$

The conditional entropy, $H(\lambda|\varphi)$, can now be obtained by using Equations 8 and 13 in Equation 3.

$$H(\lambda|\varphi) = -\int_{-\pi}^{\pi}\int_{-\pi}^{\pi} p_o[\lambda]p_1[\lambda|\varphi] \log_e p_1[\lambda|\varphi]d\varphi d\lambda \qquad 15$$

The average information transmitted per sample point (or per time interval μ) is therefore

$$\begin{array}{l}\text{Average information}\\ \text{per time interval } \mu\\ \text{in natural units}\end{array} = H(\lambda) - H(\lambda|\varphi). \qquad 16$$

Thus the average information per unit time for bandwidth W and signal-to-noise power ratio β^2 is given by

$$C_{PM} = W\left[\log_e 2\pi + \frac{1}{2\pi}\int_{-\pi}^{\pi}\int_{-\pi}^{\pi} p_1[\lambda|\varphi] \log_e p_1[\lambda|\varphi]d\lambda d\varphi\right]. \qquad 17$$

natural units per second

Information rate is more frequently referred to in bits per second. If logarithms to the base 2 had been used in Equation 17, then channel capacity would have been measured in bits per second.

$$\begin{array}{l}\text{Information rate}\\ \text{in bits per second}\end{array} = \log_2 e \begin{array}{l}\text{Information rate in}\\ \text{natural units per second}\end{array} \qquad 18$$

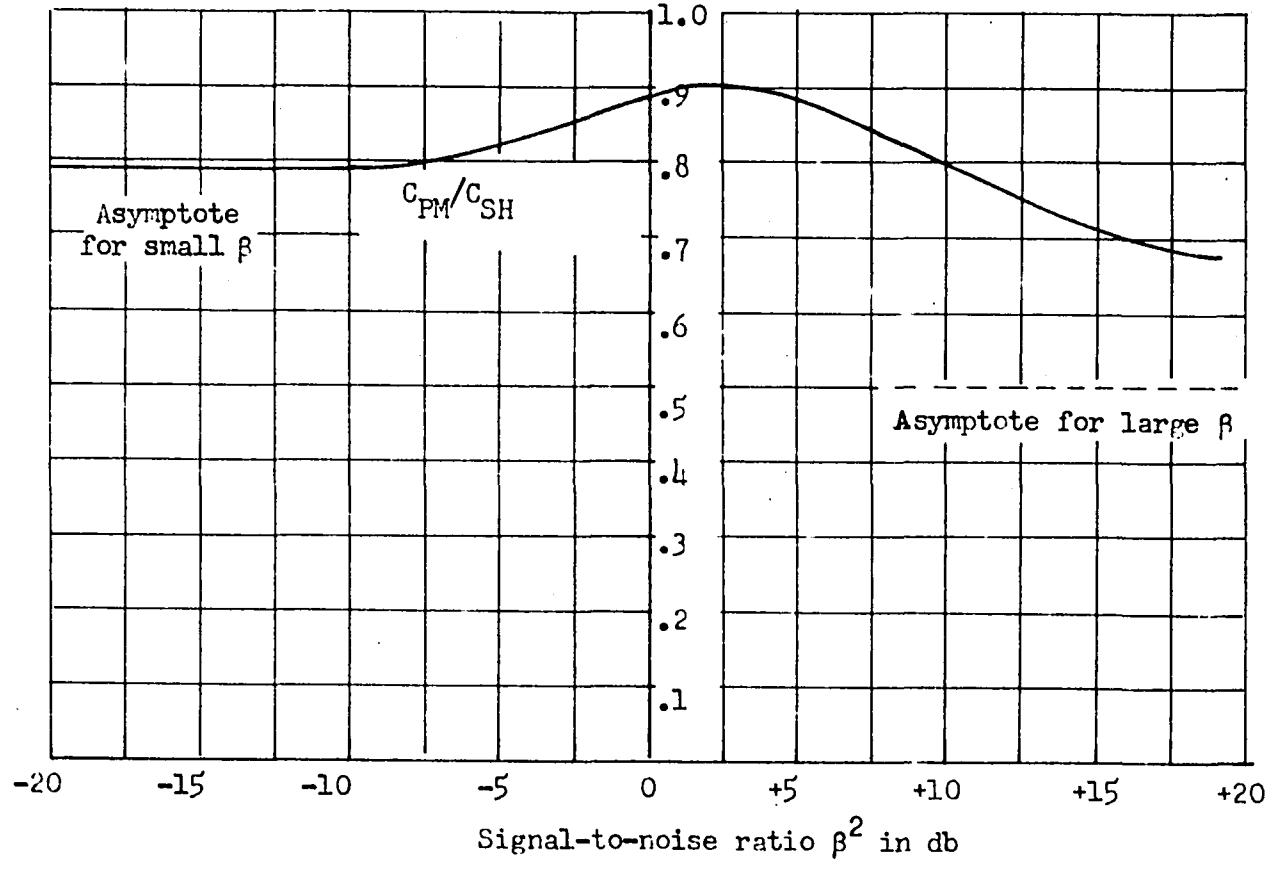

Figure 4. Plot of C_{PM}/C_{SH} as a function of β^2

It should be expected that the C_{PM} would be less than C_{SH} since the permissible signals are more restricted and thus more predictable. It should also be pointed out that C_{PM} is based on using a decoder sensitive only to phase information at sample points $\frac{1}{W}$ seconds apart. Such a decoder would be far more easily implemented than would one attempting to derive additional information from the amplitude modulation caused by the noise at the sample points.

The evaluation of Equation 17 is necessarily done numerically. Figure 4 shows the resulting plot of the ratio C_{PM}/C_{SH} as a function of β^2. The asymptotic values found by Blachman (5) are also shown. The behavior of the curve is quite unexpected between these two asymptotic values. It appears at this point, therefore, that very little sacrifice has been made by imposing the additional restrictions provided signal-to-noise ratios of less than about +10 db are used.

The amplitude function A(t) of $s_2(t)$ will be only approximately constant between sample points unlike the usual phase modulation envelope function. This will be investigated in Section III D of this paper.

The remaining portion of this paper describes the theory of operation and the calculated performance of a binary phase modulation system.

It represents an attempt to achieve performance superior to conventional amplitude, frequency, and phase modulation systems without imposing unrealistic equipment requirements.

III. PROPOSED PHASE MODULATION SYSTEM

A. Block Diagram and Mathematical Model

The basic function of a communication system is to reduce the uncertainty to the user as to the information output of the source. In this particular case, a source is postulated which generates binary information with a constant rate. This approach represents little loss in generality since a source with time varying information output rate can make use of a storage facility to maintain constant rate. Furthermore, continuous and discrete data can be converted to binary information under very general conditions provided suitable fidelity criteria are specified.

It is assumed that the source and user could communicate if the communication system were removed and the two connected directly. This permits the possibility of binary code conversions within source and user to add redundancy for purposes of error correction and detection. The function of the communication channel proposed herein is simply to transfer to the user with the greatest possible rapidity, in the narrowest possible spectrum, with the minimum possible probability of error, the binary sequence fed to its input.

Figure 5 shows the theoretical model being investigated. It represents an unusual phase modulation system for several reasons. First, the encoder is a linear device in contrast to usual practice. Second, the envelope amplitude is not constant for all values of time. Third, the cross-correlation performed upon the demodulated signal, $s_3(t)$, is not

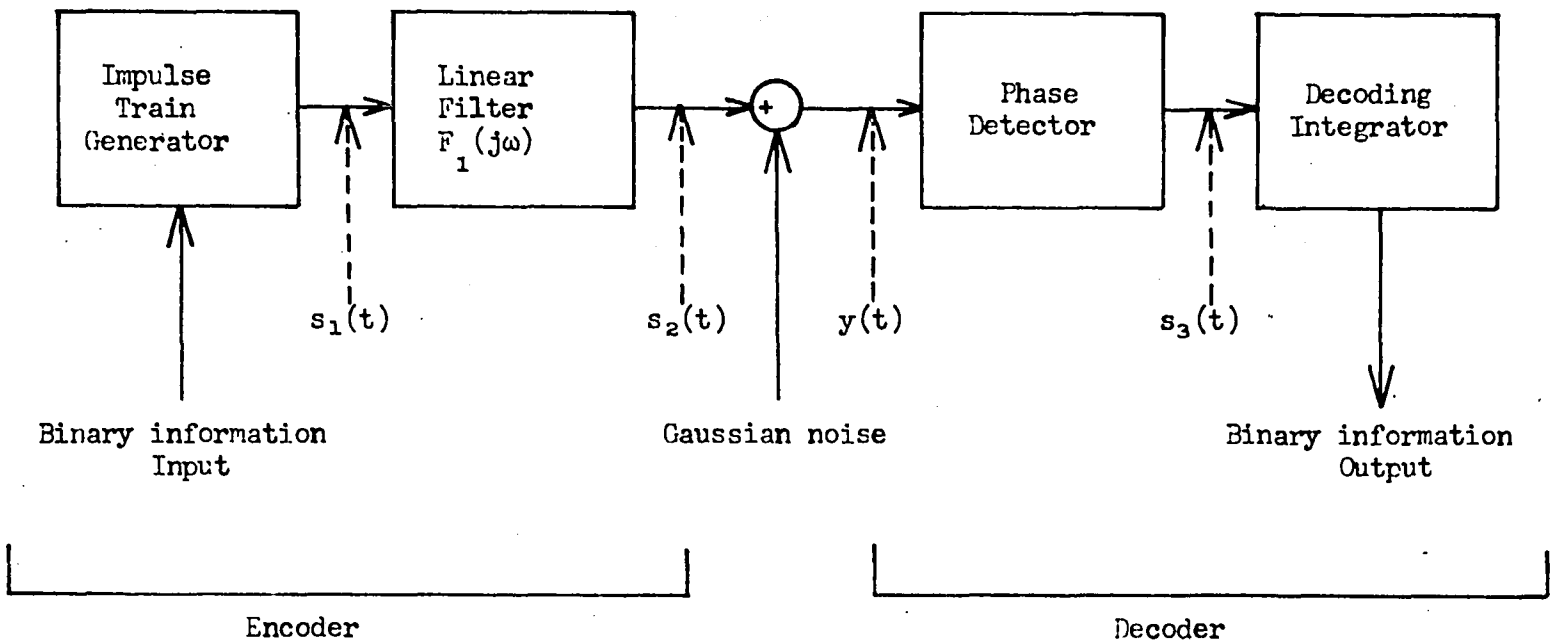

Figure 5. Diagram of proposed phase modulation system

exactly a matched filter problem as might be expected (7).

Figure 5 omits mention of any means for synchronizing the decoder to the encoder. It will become clear at a later point that this information is available to the decoder from the structure of the received signals for $n > 2$.

The block marked impulse train generator performs a coding operation. The binary input information is divided into sequential groups of length n. Consider a particular group. The n bits of information contained in this group are used to select one of 2^n sequences of regularly spaced positive and negative unit impulses. These impulses, which form $s_1(t)$, are positive or negative on the basis of an orthogonal matrix. This matrix, whose elements are all +1 or -1, is used to code the impulse train accordingly. The waveform $s_1(t)$ is, to an outside observer, an apparently random sequence of uniformly spaced positive and negative unit impulses as a result of this coding procedure.

The pseudorandom sequence of impulses regularly spaced by μ seconds is used to drive the linear filter $F_1(j\omega)$. The impulsive response of this network has been specifically chosen so that each impulse has an opportunity to control the output phase of $s_2(t)$ at a particular instant in time. At these particular time points, called sample points hereafter, the envelope amplitude is always A but the relative phase λ is $\pm \frac{\pi}{2}$ radians depending upon the polarity of the corresponding unit impulse.

The narrowband, white, gaussian noise waveform, $\alpha(t)$, is presumed to occupy the same bandwidth as the spectrum of the decoder output. It is simply added to $s_2(t)$ to form $y(t)$.

$$y(t) = s_2(t) + \alpha(t) \qquad 19$$

The phase detector is responsive only to the slowly varying phase of $y(t)$. As will be defined later, its output is directly proportional to $\varphi(t)$.

The block marked decoding integrator estimates which of the 2^n impulse trains was actually sent. In this paper, all of them are considered a priori equiprobable. The time function $s_3(t)$ is sampled at the 2^{n-1} points μ seconds apart which represent the unique sample points mentioned earlier. On the basis of 2^n correlators acting upon these 2^{n-1} samples a decision can be reached as to the most probably transmitted binary group. This study is principally devoted to determining the rate of error and information flow at the output of this decision device.

B. Theory of Encoder Operation

As mentioned earlier, Woodward (2) has shown that cross-correlation is the optimum basis for decision concerning known waveforms received through additive, gaussian noise. However, in this particular problem, the noise is not gaussian at the output of the phase detector even though gaussian noise was added to the output of the encoder. Nevertheless, for values of $\beta > 1$ the function $p_1[\lambda|\varphi]$ is reasonably similar to a gaussian probability density function. It is, however, virtually impossible to devise a matched filter for the proposed system to permit the optimum decision process to be instrumented for the proposed system. As a result of these considerations, waveforms orthogonal to each other at the sample points and sample point decoding based on cross-correlation will be em-

ployed. A code based on Hadamard matrices, $\overline{H}_k$, was selected for use (8). Figure 6a shows a 2 x 2 Hadamard matrix.

Hadamard matrices are orthogonal matrices having as elements +1 or -1. These matrices have the interesting property that

$$\overline{H}_{2k} = \begin{bmatrix} \overline{H}_k & \overline{H}_k \\ \overline{H}_k & -\overline{H}_k \end{bmatrix} \qquad 20$$

This property shows how to construct a 2k x 2k matrix given a k x k matrix. Figure 6b shows its use upon a 2 x 2 matrix. All 4k x 4k Hadamard matrices for k = 1, 2, - - - - 28 are known to exist (8). This fact may be used for the construction of systems with non-integer values of n. To construct the code using, for example, n = 3 a 4 x 4 Hadamard matrix and its negative is employed. Each of the eight rows which results is used as a code symbol for later conversion to an impulse train. Figure 7 shows the coding correspondence. All of the remaining code symbols are orthogonal to any one particular code symbol with the exception of one which is strictly negative. It is apparent that as n increases the code symbols will become exponentially longer than the binary sequences they represent. In this way more redundancy is added at the expense of information rate to decrease the rate of erroneous decision at the decoder.

Through the use of Equation 20, 2 x 2, 4 x 4, 8 x 8, and 16 x 16 Hadamard matrices are readily obtained. A 12 x 12 matrix is shown in Figure 8 for completeness in low values of matrix order (9). This 12 x 12 matrix would lead to n = 4.58.

$$\begin{bmatrix} +1 & +1 \\ +1 & -1 \end{bmatrix}$$

(a)

$$\begin{bmatrix} +1 & +1 & +1 & +1 \\ +1 & -1 & +1 & -1 \\ +1 & +1 & -1 & -1 \\ +1 & -1 & -1 & +1 \end{bmatrix}$$

(b)

Figure 6. Examples of Hadamard matrices

Binary sequence	Hadamard code symbol
000	+1 +1 +1 +1
001	+1 -1 +1 -1
010	+1 +1 -1 -1
011	+1 -1 -1 +1
100	-1 -1 -1 -1
101	-1 +1 -1 +1
110	-1 -1 +1 +1
111	-1 +1 +1 -1

Figure 7. Hadamard code for n = 3

$$
\begin{bmatrix}
+1 & +1 & +1 & +1 & +1 & +1 & +1 & +1 & +1 & +1 & +1 & +1 \\
+1 & -1 & +1 & -1 & +1 & +1 & +1 & -1 & -1 & -1 & +1 & -1 \\
+1 & -1 & -1 & +1 & -1 & +1 & +1 & +1 & -1 & -1 & -1 & +1 \\
+1 & +1 & -1 & -1 & +1 & -1 & +1 & +1 & +1 & -1 & -1 & -1 \\
+1 & -1 & +1 & -1 & -1 & +1 & -1 & +1 & +1 & +1 & -1 & -1 \\
+1 & -1 & -1 & +1 & -1 & -1 & +1 & -1 & +1 & +1 & +1 & -1 \\
+1 & -1 & -1 & -1 & +1 & -1 & -1 & +1 & -1 & +1 & +1 & +1 \\
+1 & +1 & -1 & -1 & -1 & +1 & -1 & -1 & +1 & -1 & +1 & +1 \\
+1 & +1 & +1 & -1 & -1 & -1 & +1 & -1 & -1 & +1 & -1 & +1 \\
+1 & +1 & +1 & +1 & -1 & -1 & -1 & +1 & -1 & -1 & +1 & -1 \\
+1 & -1 & +1 & +1 & +1 & -1 & -1 & -1 & +1 & -1 & -1 & +1 \\
+1 & +1 & +1 & +1 & +1 & +1 & -1 & -1 & -1 & +1 & -1 & -1
\end{bmatrix}
$$

Figure 8. 12 x 12 Hadamard Matrix

Figure 9 shows an example of $s_1(t)$ which would correspond to a typical binary sequence using the code shown in Figure 7.

The series of positive and negative impulse functions, designated $s_1(t)$, is used to drive a linear network. This network has an impulse response

$$f_1(t) = \frac{\sin \frac{\pi}{\mu}(t - 5\mu) \cos \omega_o t}{\frac{\pi}{\mu}(t - 5\mu)} [u_1(t) - u_1(t - 10\mu)]. \qquad 21$$

This function is sketched in Figure 10 under the assumption that $\omega_o >> \frac{\pi}{\mu}$.

The impulse response shown in Equation 21 is perhaps most easily realized through the use of a truncated $\frac{\sin x}{x}$ function as given by

$$\hat{f}_1(t) = \frac{\sin \frac{\pi}{\mu}(t - 5\mu)}{\frac{\pi}{\mu}(t - 5\mu)} [u_1(t) - u_1(t - 10\mu)]. \qquad 22$$

This more easily realizable impulse response can then be fed to a balanced modulator operating at angular frequency ω_o to obtain $f_1(t)$. Figure 11 shows a sketch of $\hat{f}_1(t)$.

C. Derivation of Spectrum Bandwidth

The impulse response given by Equation 21 represents a finite portion of the sampling function discussed in Appendix B. In order to ascertain the output spectrum of the encoder, it is necessary to determine the autocorrelation function of $s_1(t)$. The Fourier transform of the autocorrelation function determines the power density spectrum at the input of the linear filter $F_1(j\omega)$. The function $S_2(j\omega)$ is then available. It represents the spectrum of the encoder output.

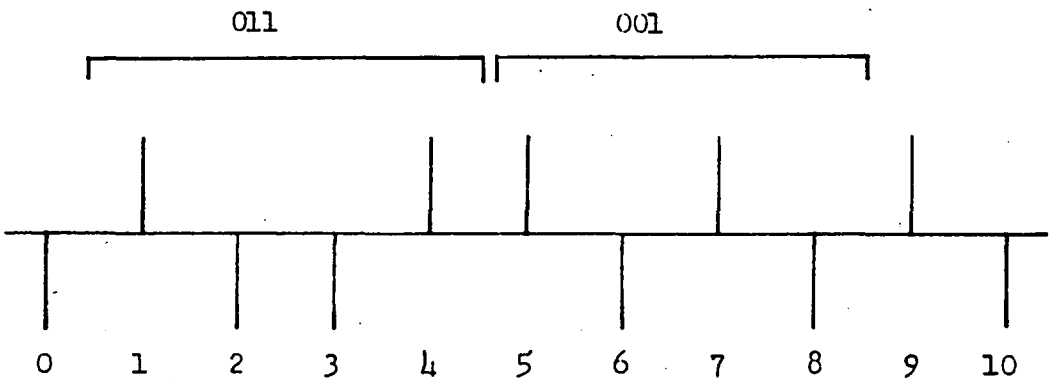

Figure 9. An example of $s_1(t)$ with corresponding binary sequence

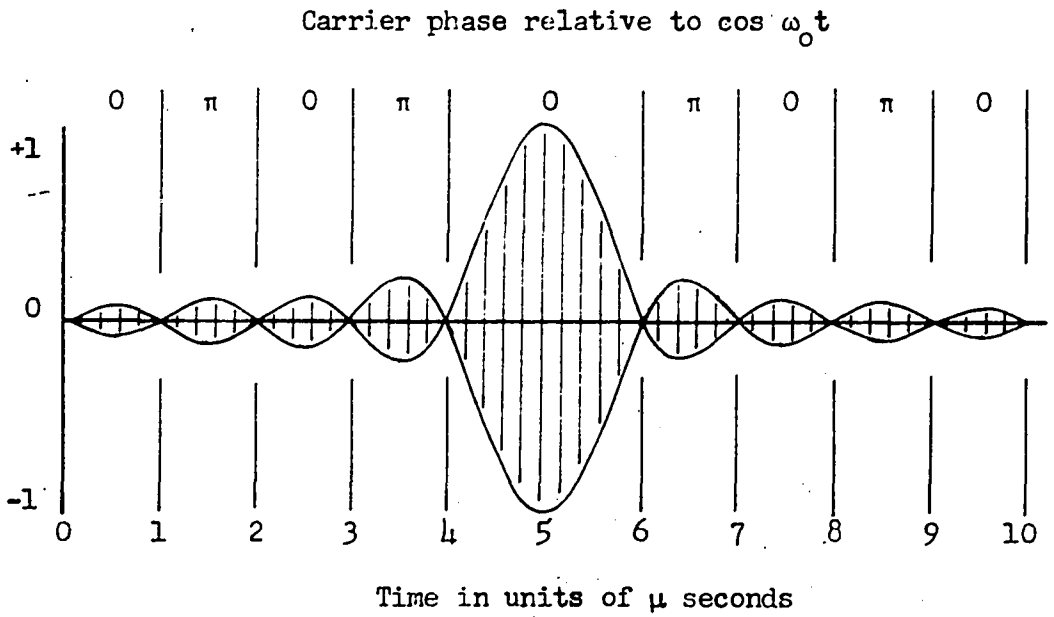

Figure 10. Sketch of function given by equation 21

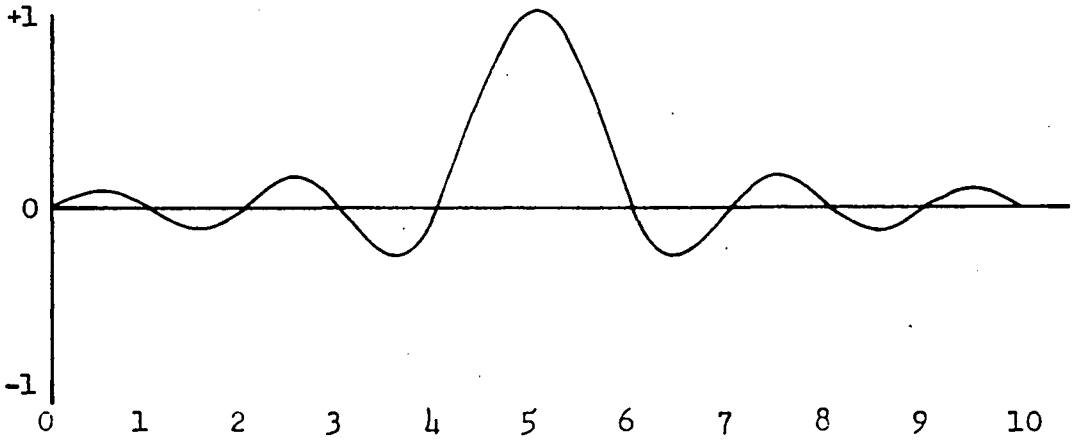

Figure 11. Sketch of $\hat{f}_1(t)$ as given by equation 22

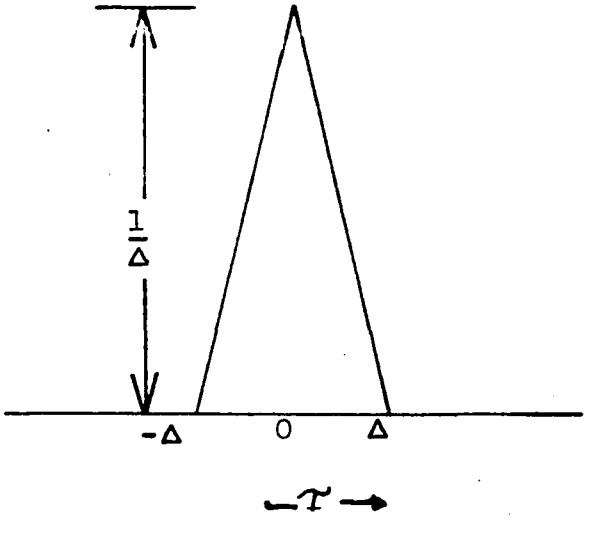

Figure 12. Autocorrelation function of rectangular pulse of width Δ

The limiting autocorrelation function of $s_1(t)$ will be obtained by temporarily letting each unit impulse be replaced by a rectangular pulse of width Δ and height $\frac{1}{\Delta}$ seconds. The function $s_1(t)$ thus becomes a pseudorandom sequence of finite rectangular pulses each having unit area. Equation 20 shows that if a code is devised in the manner prescribed, knowledge of the algebraic sign of one code symbol element tells nothing about the polarity of any other element, adjacent or otherwise. This fact is described by

$$\text{Probability}\left\{\text{element } (i,j) = +1 \,\middle|\, \text{element } (i,k) = \pm 1, j \neq k\right\} = \frac{1}{2}. \qquad 23$$

This equation refers to the enlarged 2k x k matrix consisting of a k x k Hadamard matrix and its negative. Therefore, the autocorrelation function, defined by

$$R(\tau) = \lim_{T\to\infty} \frac{1}{2T} \int_{-T}^{T} s_1(t)s_1(t+\tau)dt \qquad 24$$

of the rectangular pulse function is shown in Figure 12. If the limiting operation in Δ is now performed, Equation 25 will give the autocorrelation function.

$$\lim_{\Delta\to 0} R(\tau) = u_o(\tau) \qquad 25$$

The Fourier transform of $s_1(t)$ is

$$S_1(j\omega) = \int_{-\infty}^{\infty} s_1(t) \exp(-j\omega t)dt. \qquad 26$$

The power density spectrum at the input to $F_1(j\omega)$ is (10) the Fourier transform of $R(\tau)$.

$$\left|S_1(j\omega)\right|^2 = \int_{-\infty}^{\infty} R_1(\tau) \exp(-j\omega\tau)d\tau = 1 \qquad 27$$

The limiting Fourier transform of the unit impulse function $u_o(\tau)$ is given by

$$S_1(j\omega) = 1. \tag{28}$$

Consequently, the complex spectrum

$$S_2(j\omega) = F_1(j\omega)S_1(j\omega) = F_1(j\omega). \tag{29}$$

The function $F_1(j\omega)$ is obtained by use of Equations 21 and 30.

$$F_1(j\omega) = \int_{-\infty}^{\infty} f_1(t) \exp(-j\omega t)dt \tag{30}$$

Equation 30 may be evaluated by using several properties of Fourier transforms. First, change the variable t to

$$\hat{t} = t - 5\mu. \tag{31}$$

Upon substituting Equation 31 into Equation 30, $F_1(j\omega)$ becomes

$$F_1(j\omega) = \exp(-j5\omega\mu) \int_{-\infty}^{\infty} f_1(\hat{t} + 5\mu) \exp(-j\omega\hat{t})d\hat{t}. \tag{32}$$

The use of Equation 21 in Equation 32 leads to

$$F_1(j\omega) = \frac{\exp(-j5\omega\mu)}{2} \int_{-\infty}^{\infty} [\exp(j\omega_o\hat{t} + j5\mu\omega_o) + \exp(-j\omega_o\hat{t} - j\omega_o 5\mu)] \frac{\sin\frac{\pi\hat{t}}{\mu}}{\frac{\pi\hat{t}}{\mu}} [u_1(\hat{t} + 5\mu) - u_1(\hat{t} - 5\mu)] \exp(-j\omega\hat{t})d\hat{t}. \tag{33}$$

Equation 33 may be simplified through use of the property of Fourier transforms given by Equation 34.

$$\int_{-\infty}^{\infty} f(t) \exp(j\omega_o t) \exp(-j\omega t)dt = F(j(\omega - \omega_o))$$

$$\int_{-\infty}^{\infty} f(t) \exp(-j\omega t)dt = F(j\omega) \tag{34}$$

Consequently, evaluation of the transform of Equation 33 is basically a problem of evaluating integral $I_1(j\omega)$ as defined by

$$I_1(j\omega) = \int_{-\infty}^{\infty} \frac{\sin \frac{\pi}{\mu} \hat{t}}{\frac{\pi}{\mu} \hat{t}} [u_1(\hat{t} + 5\mu) - u_1(\hat{t} - 5\mu)] \exp(-j\omega\hat{t}) d\hat{t}. \qquad 35$$

This integral, in turn, is considered to be the transform of a product of functions resulting in the use of complex convolution.

$$I_1(j\omega) = \frac{5}{\pi} \mu^2 \int_{-\infty}^{\infty} \frac{\sin 5v\mu}{5v\mu} [u_1(\omega - v + \frac{\pi}{\mu}) - u_1(\omega - v - \frac{\pi}{\mu})] \, dv \qquad 36$$

The exponential factors found in Equation 33 will not change the spectrum magnitude as a function of frequency. The translation property expressed by Equation 34 means that the complex function shown in Equation 36 is actually centered at frequencies $\pm \omega_o$. If $\omega_o >> \frac{\pi}{\mu}$, the two complex spectra which are respectively centered at $\pm \omega_o$ will not significantly overlap. Figure 13 shows the plot of the magnitude of the spectrum, $S_2(j\omega)$, which results from Equation 33. The integral in Equation 36 was evaluated through the use of Si(x) tables (11).

Figure 13 also shows the spectrum magnitude which is attainable using the sampling theory outlined in Appendix B. Apparently the sacrifice made by truncating the sampling function at the $\pm 5\mu$ points is not large. The 5μ second delay imposed to ensure physical realizability does not affect the magnitude of the spectrum.

The output function $s_2(t)$ is therefore enclosed by an envelope having a fixed amplitude at sample points which are μ seconds apart. In the next section, the statistical behavior of the envelope amplitude be-

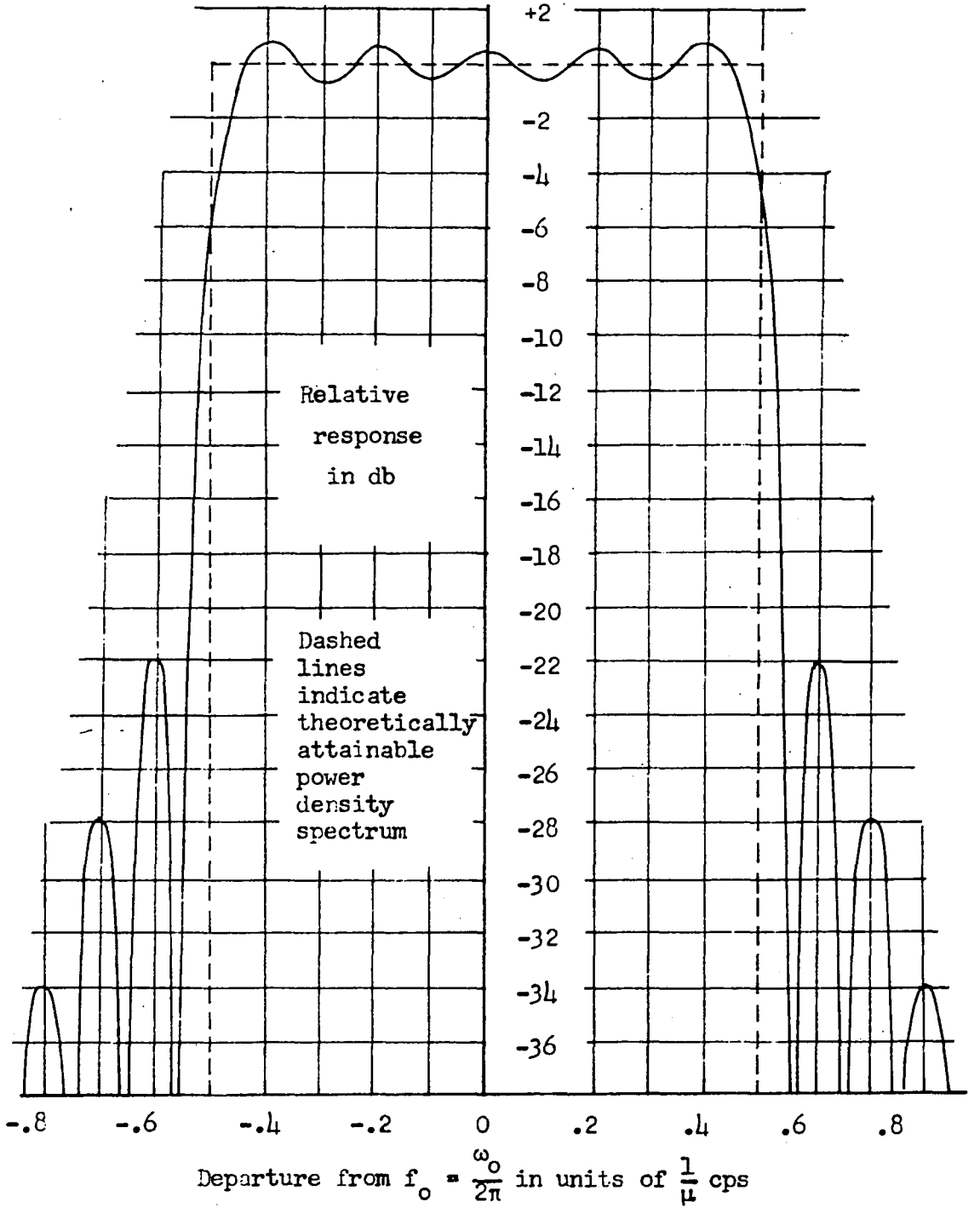

Figure 13. Power density spectrum of $S_2(j\omega)$

tween sample points is studied.

D. Encoder Output Envelope Amplitude Probability Distribution Function

The impulse response function $f_1(t)$ has a total duration of 10μ seconds. At any particular instant, the envelope amplitude of $s_2(t)$ is influenced by the polarity of 10 unit impulses. In the binary case being investigated the summation of the contributions of the 10 sample functions is purely algebraic. However, the obvious extension of this work to non-binary phase modulation will require component summation on a vectorial basis.

Suppose that the +1 elements in the 2k x k modified Hadamard matrices correspond to sample point phases of $+\frac{\pi}{2}$ with respect to $\sin \omega_o t$. In like manner, the -1 elements correspond to $-\frac{\pi}{2}$ phases at sample points. Since these two phases are maximally separated the rate of decoder error will be less than for any other phase change equal to less than π radians. However, this phase separation has the unfortunate effect of causing the envelope to vary quite greatly between sample points. Since only 10 unit impulses can influence the envelope amplitude at any particular instant, it is possible to determine its probability distribution function as a function of location between sample points. This study was conducted using the random nature of the impulse polarities and the impulse response given by Equation 21. The 2^{10} possible combinations were considered equally probable. The 10 impulse functions influencing the amplitude were then properly weighted. The results are shown in Figure 14. The proba-

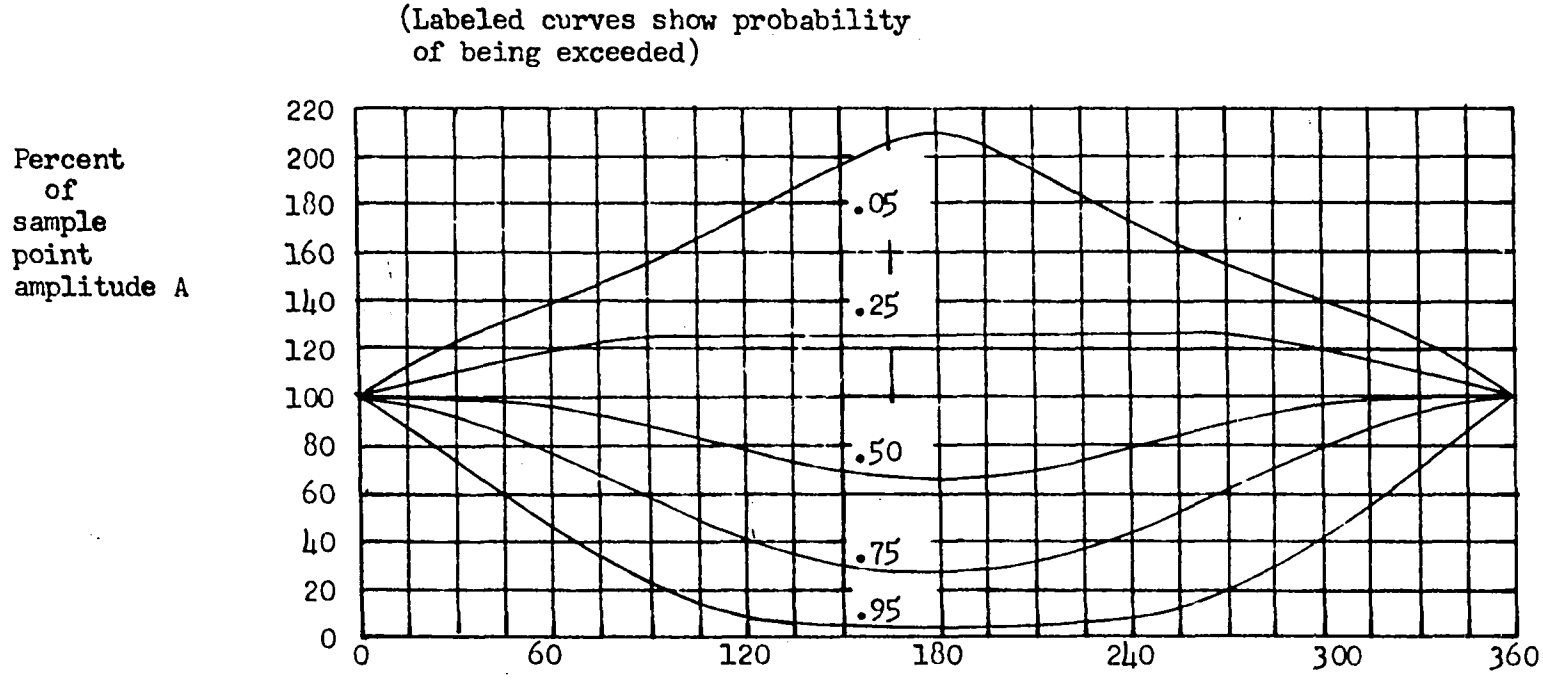

Figure 14. Probability contours for envelope probability distribution functions between sample points

bility contours represent the probability that the envelope amplitude will exceed the relative magnitude shown in terms of A. The value A is the sample point envelope amplitude.

E. Theory of Decoder Operation

The decoder must base its decisions completely upon the waveform $y(t)$. In particular, the decisions made every $2^{n-1}\mu$ seconds are based upon the received signal phase φ at the 2^{n-1} sample points corresponding to a code symbol sent by the encoder. The parameter β^2 representing signal-to-noise power ratio at the sample points, will strongly influence the accuracy with which the decisions can be made.

The noisy signal waveform, $y(t)$, will have a slowly varying phase function since both the signal, $s_2(t)$, and noise, $\alpha(t)$, are narrowband waveforms. This combination is operated upon by the phase detector as shown by Figure 5. This detector is assumed responsive to phase only. Its transfer function is shown in Figure 15. This curve represents the output voltage or current resulting from an input phase φ in the range $-\pi \leq \varphi \leq \pi$ radians.

It is, of course, necessary to provide the phase detector with a reference signal against which it can determine the sample point phase. This detail has been omitted from Figure 5. However, through the use of frequency multipliers and phase locked servomechanisms this reference signal can be provided.

Under noise-free conditions ($\beta^2 = \infty$) the output of the phase detector will be an irregular rectangular pulse waveform. The detector

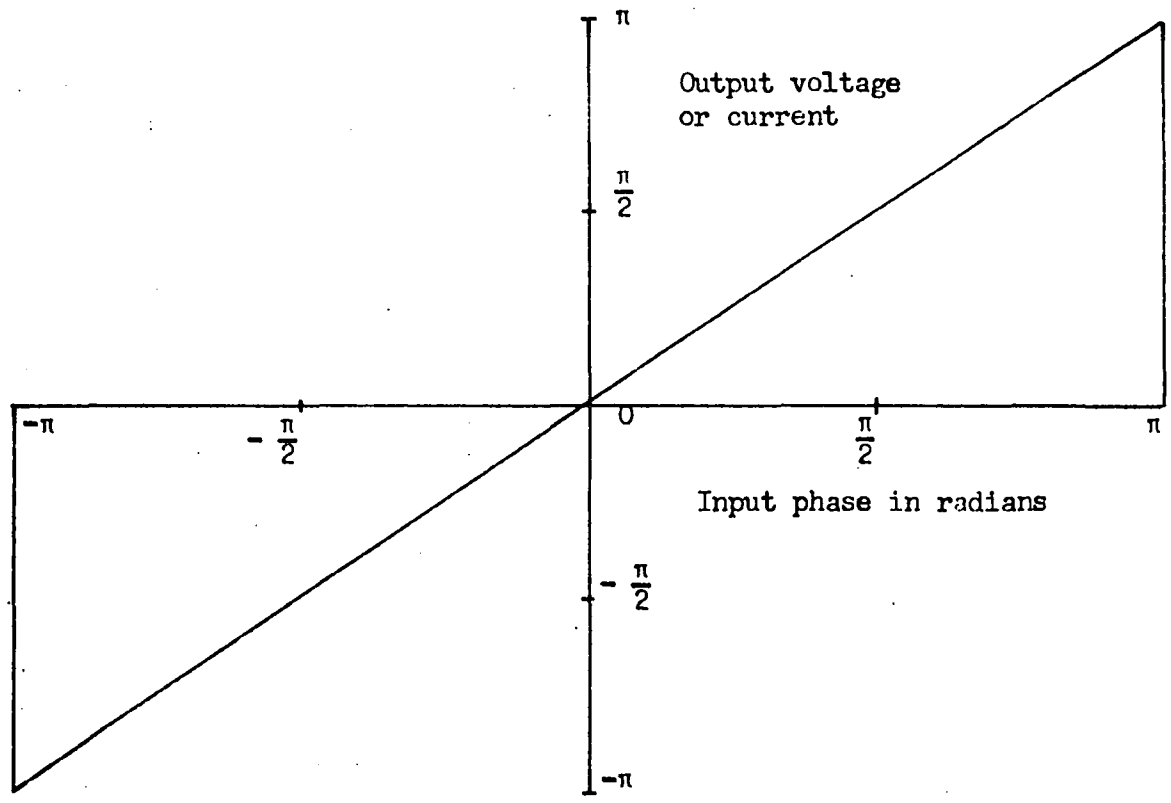

Figure 15. Transfer function of the phase detector

output will be $\pm \frac{\pi}{2}$ at the sample points depending upon transmitted phase λ. At the other extreme, when $\beta^2 = 0$, the waveform fed out of the detector will be non-gaussian noise whose probability density function is

$$p_1[\varphi|\lambda] = \frac{1}{2\pi}. \qquad 37$$

$$-\pi \leq \varphi \leq \pi.$$

The waveform at the output of the phase detector will be operated upon by the decoding integrator. This device performs the operation of cross-correlation in a discrete sense upon the 2^{n-1} sample points in the code symbol being decoded. Actually, 2^n such cross-correlators simultaneously examine each demodulated waveform. Under noiseless conditions, the output of the correlator corresponding to the code symbol actually transmitted will be

$$x_1 = 2^{n-1} \frac{\pi}{2}. \qquad 38$$

In all of the work which follows, this output signal will be designated x_1.

The output of the correlator corresponding to the negative of the actually transmitted code symbol will be called x_2. All other correlators corresponding to code symbols orthogonal to x_1 and x_2 and have outputs designated as x_3, x_4, x_5 - - - - - x_2^n. It will be assumed that x_4 is the negative of x_3, etc. The probability density function at these outputs orthogonal to x_1 will all be the same as that for x_3.

Obviously the output of x_2 is negative to that of x_1 even under noisy conditions of operation. For the remaining 2^n -2 correlators, the output signal x_i will, in general, be zero only for noiseless con-

ditions. This is basically due to the fact that any two orthogonal code symbols have as many equal as opposite algebraic signs. (See Figure 7, for example.)

The decoder bases its decision as to which code symbol was most probably transmitted upon which of the 2^n cross-correlators produces the largest positive output signal x. In the next section, equations are derived which describe the probability density functions on these 2^n correlator outputs.

F. Decoder Output Probability Density Functions

The probability density function describing the output of the phase detector at a sample point for which the transmitted phase λ was $\frac{\pi}{2}$ is

$$p_1[\varphi|\tfrac{\pi}{2}] = \frac{\exp(-\beta^2)}{2\pi} + \frac{\beta\cos(\varphi - \frac{\pi}{2})}{\sqrt{\pi}} \exp\left[-\beta^2 \sin^2(\varphi - \tfrac{\pi}{2})\right] \frac{1}{\sqrt{2\pi}} \int_{-\infty}^{\sqrt{2}\beta\cos(\varphi - \frac{\pi}{2})} \exp -\frac{t^2}{2}\, dt. \qquad 39$$

$$-\pi \leq \varphi \leq \pi.$$

For the simple case when n = 1 there is only one sample point per code symbol. The probability density function describing the output x_1 is therefore

$$P_1^{(1)}[x_1;\beta] = p_1[x_1|\tfrac{\pi}{2}]. \qquad 40$$

The corresponding density function $P_2^{(1)}[x_2;\beta]$ for the output signal x_2 is exactly the same except that x_1 in Equation 40 is replaced by $-x_2$.

$$P_2^{(1)}[x_2;\beta] = p_1[-x_2|\tfrac{\pi}{2}] \qquad 41$$

Through the use of the sampling theory of Appendix B it is known that the narrowband noise waveform, $\alpha(t)$, has independent phase values at time intervals separated by μ seconds. Therefore, in the case of $n = 2$, the two probability density functions at the two sample points correspond to two independent random variables. This permits the density function describing their sum to be found by convolution (10). Thus for $n = 2$, the density function for x_1 is

$$P_1^{(2)}[x_1;\beta] = \int_{-2\pi}^{2\pi} P_1^{(1)}[z;\beta]P_1^{(1)}[x_1 - z;\beta]dz. \qquad 42$$

$$-2\pi \leq x_1 \leq 2\pi.$$

The function $P_2^{(2)}[x_2;\beta]$ can be obtained from Equation 42 by replacing x_1 by $-x_2$.

The probability density function for x_3 when $n = 2$ must also be obtained by convolution. Here, however, it should be recalled that one of the two sample points tends to be $+\frac{\pi}{2}$ while the other tends to be $-\frac{\pi}{2}$. Therefore, it may be expected that the two orthogonal outputs will have zero mean values. The result is

$$P_3^{(2)}[x_3;\beta] = \int_{-2\pi}^{2\pi} P_1^{(1)}[z;\beta]P_2^{(1)}[x_3 - z;\beta]dz. \qquad 43$$

$$-2\pi \leq x_3 \leq 2\pi.$$

For the case of $n = 3$, four sample points influence the correlator outputs. The probability density function for x_1 is

$$P_1^{(3)}[x_1;\beta] = \int_{-4\pi}^{4\pi} P_1^{(2)}[z;\beta]P_1^{(2)}[x_1 - z;\beta]dz. \qquad 44$$

$$-4\pi \leq x_1 \leq 4\pi.$$

The function $P_2^{(3)}[x_2;\beta]$ can be obtained from Equation 44 by replacing x_1 with $-x_2$.

The function $P_3^{(3)}[x_3;\beta]$ is obtained by convolution of two previously derived probability density functions as shown in Equation 45.

$$P_3^{(3)}[x_3;\beta] = \int_{-4\pi}^{4\pi} P_1^{(2)}[z;\beta]P_2^{(2)}[x_3 - z;\beta]dz \qquad 45$$

$$-4\pi \leq x_3 \leq 4\pi$$

The general formulas are now apparent.

$$P_1^{(n)}[x_1;\beta] = \int_{-2^{n-1}\pi}^{2^{n-1}\pi} P_1^{(n-1)}[z;\beta]P_1^{(n-1)}[x_1 - z;\beta]dz. \qquad 46$$

$$-2^{n-1}\pi \leq x_1 \leq 2^{n-1}\pi.$$

$$P_2^{(n)}[x_2;\beta] = P_1^{(n)}[-x_1;\beta] \qquad 47$$

$$P_3^{(n)}[x_3;\beta] = \int_{-2^{n-1}\pi}^{2^{n-1}\pi} P_1^{(n-1)}[z;\beta]P_2^{(n-1)}[x_3 - z;\beta]dz. \qquad 48$$

$$-2^{n-1}\pi \leq x_3 \leq 2^{n-1}\pi.$$

These probability density functions will be used in the next section to obtain the expressions specifying rate of error committed by the decoder due to noise interference.

IV. ERROR RATE PERFORMANCE OF PROPOSED SYSTEM

The decoder makes a correct decision as to which code symbol was actually sent only if x_1 is greater than all other output signals. Obviously this is impossible if the value of x_1 is negative since in that event x_2 would be positive and therefore greater.

In the case of n = 1, the probability of correct decoding is

$$P_C^{(1)}[\beta] = \int_0^{\pi} P_1^{(1)}[x_1;\beta]dx_1. \tag{46}$$

For n = 2, recognition must be made of the fact that for correct decision to be made x_1 must be greater than x_3 and x_4 as well as x_2. This is properly expressed by

$$P_C^{(2)}[\beta] = \int_0^{2\pi} P_1^{(2)}[x_1;\beta]\left\{\int_{-x_1}^{x_1} P_3^{(2)}[x_3;\beta]dx_3\right\}dx_1. \tag{47}$$

The limits on the inner integral assure that both x_3 and x_4 are less than x_1. The lower limit of zero on the outer integral precludes x_2 being greater than x_1.

When n = 3, three orthogonal code symbol pairs must be considered. It is necessary that all of these six outputs be simultaneously less than x_1. Equation 48 shows the relation appropriate to the probability of correct decoding in this instance.

$$P_C^{(3)}[\beta] = \int_0^{4\pi} P_1^{(3)}[x_1;\beta]\left\{\int_{-x_1}^{x_1} P_3^{(3)}[x_3;\beta]dx_3\right\}^3 dx_1 \tag{48}$$

It should be recalled here that all of the other orthogonal outputs have the same probability density as x_3 and therefore $P_3^{(n)}[x_3;\beta]$ may be used

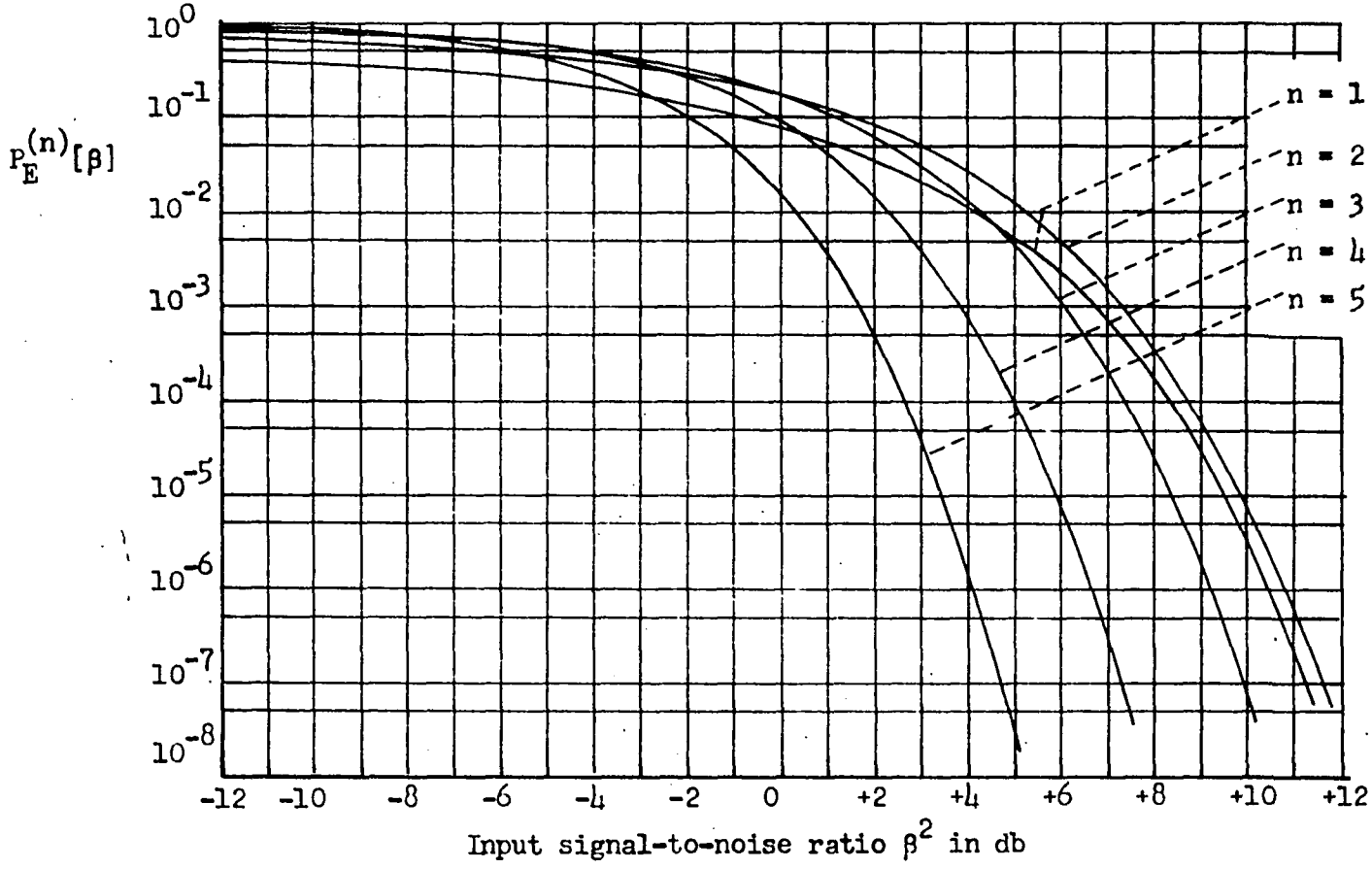

Figure 16. Plot of $P_E^{(n)}[\beta]$ for several values of parameter n

instead.

The general formula for the probability of correct decision when n bits per code symbol and a signal-to-noise power ratio β^2 is used becomes

$$P_C^{(n)}[\beta] = \int_0^{2^{n-1}\pi} P_1^{(n)}[x_1;\beta]\left\{\int_{-x_1}^{x_1} P_3^{(n)}[x_3;\beta]dx_3\right\}^{2^{n-1}-1} dx_1. \qquad 49$$

$$n = 1, 2, - - - - -.$$

The probability of error is designated $P_E^{(n)}[\beta]$.

$$P_E^{(n)}[\beta] = 1 - P_C^{(n)}[\beta] \qquad 50$$

Error rate computations have been made using a digital computer. This work was done using 12 values of β over n = 1, 2, 3, 4, and 5. Figure 16 shows the plotted results.

V. CHANNEL EFFICIENCY OF PROPOSED SYSTEM

The data plotted in Figure 16 makes it possible to compute the rate of information flow, C_x, through the communication system. To calculate C_x the system will be considered a noisy discrete channel from the viewpoint of the binary input and output terminals.

The transition probabilities are not easily determined, however. This difficulty is due to the much greater likelihood of erroneous choice of $x_3 \ldots x_{2n}$ than of x_2. Since the orthogonal code symbols all have zero cross-correlation with the actually transmitted signal, the transition to $x_3 \ldots x_{2n}$ will be considered equally likely. Because of the large negative cross-correlation of the transmitted code symbol with its negative, x_2 will be considered as having zero probability of occurrence except in the case of n = 1. The transition probabilities to orthogonal code symbols will, therefore, be given by

$$\text{Transition probability to } x_3, \text{ - - - - } x_{2n} = \frac{P_E^{(n)}[\beta]}{2^n - 2}. \qquad 51$$

Using the noisy, discrete channel approach (12) leads to a formula for C_x given by

$$C_x = \frac{n + P_C^{(n)}[\beta]\log_2 P_C^{(n)}[\beta] + P_E^{(n)}[\beta]\log_2 \dfrac{P_E^{(n)}[\beta]}{2^n - 2}}{2^{n-1}\mu} \qquad 52$$

bits per second.

Figure 17 shows a plot of C_x/C_{SH}. These curves show the relative efficiency of this communication system as compared to the ideal Shannon

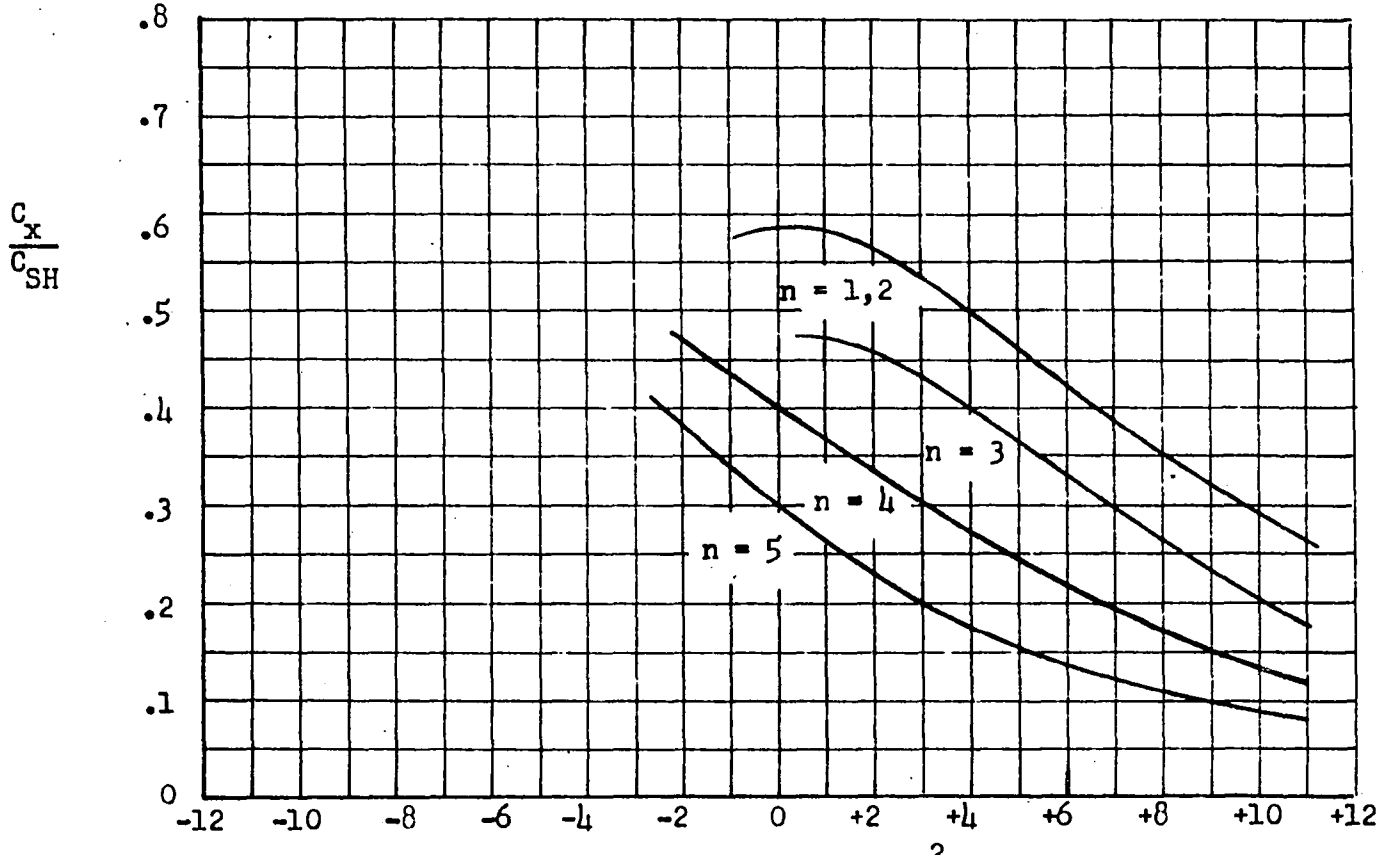

Figure 17. Plot of C_x/C_{SH} as a function of β^2

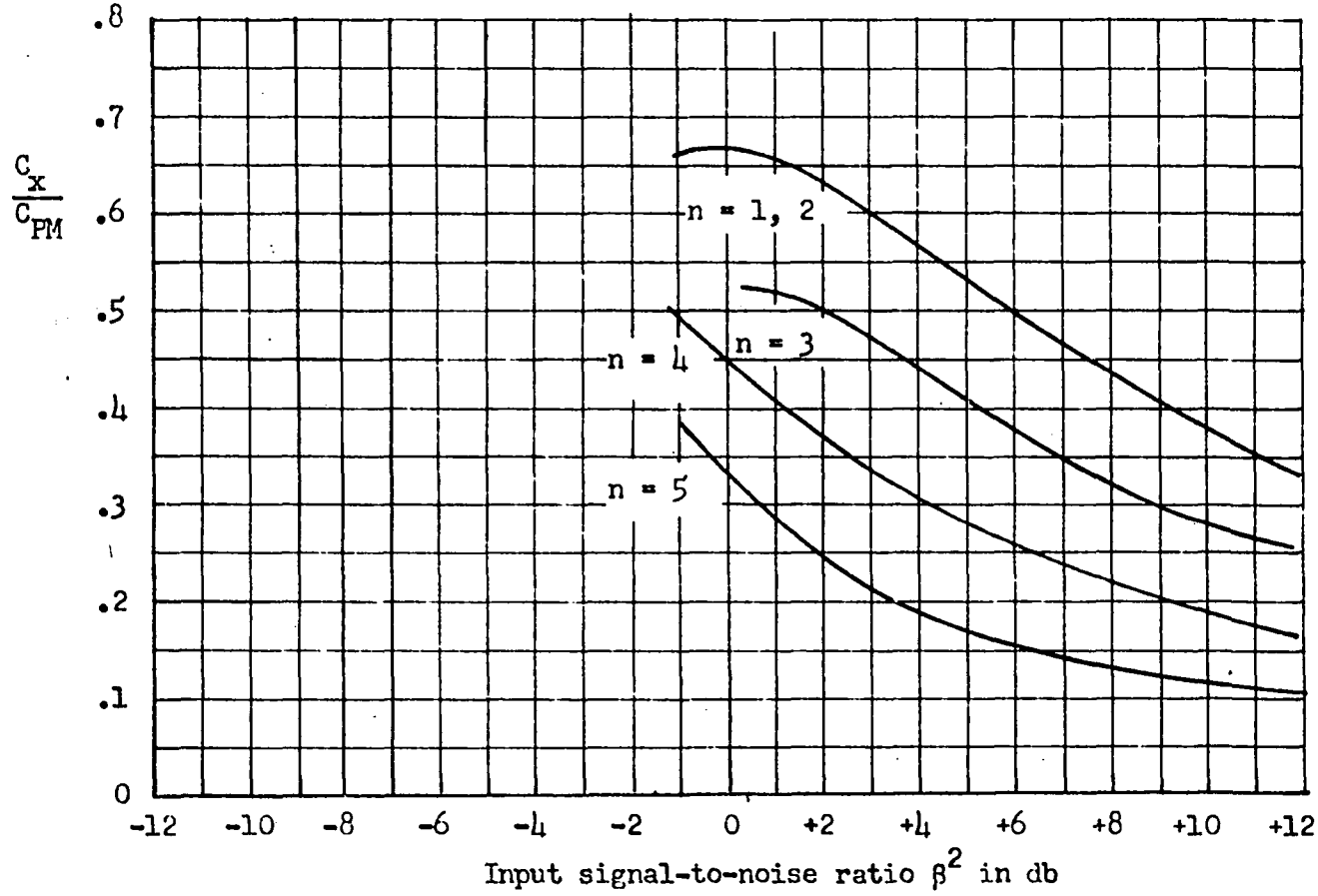

Figure 18. Plot of C_x/C_{PM} as a function of β^2

channel.

Figure 18 shows the ratio C_x/C_{PM}. These curves show the extent to which this system approaches what can be done with purely phase modulated systems.

These two curves are discussed in the next section.

VI. DISCUSSION AND SUMMARY

Basically, the data for Figures 17 and 18 are obtained from Figure 16. These data could actually be presented in numerous additional ways since there are several interrelated variables. For instance, sample point signal-to-noise ratio β^2, bandwidth W, error rate $P_E^{(n)}[\beta]$, information rate C_x, and coding parameter n are variables important in the design of this type of communication system. By way of illustration two examples of system designs will be discussed. In both examples, two systems (system 1 and system 5) will be discussed. System 1 will use n = 1 while system 5 will employ n = 5. The first example will show how bandwidth W vs. error rate $P_E^{(n)}[\beta]$ may be computed while using constant sample point encoder amplitude A and constant information rate C_x.

Refer to Figure 16. Note that in order for $P_E^{(n)}[\beta]$ to be 10^{-6}, β^2 must be 10.4 db for n = 1. In order to transmit information at the same rate with n = 5, it is necessary to send $\frac{16}{5}$ times as many sample points per second. This means that in order to maintain the same rate of flow of information in system 5 it is necessary to increase the bandwidth by $\frac{16}{5}$ over what is needed by system 1. However, if we also assume that the noise power spectral density is fixed and independent of frequency the value of β^2 becomes (10.4 - 5.05) db = 5.35 db for the case of n = 5. Note, however, that the error rate is less than 10^{-8} in this case. Consequently, in exchange for the use of more bandwidth an improved error rate is obtained.

For the second example it will be assumed that system 1 and system 5

both operate with an error rate of 10^{-5}. In the case of system 1 the value of β^2 must be 9.4 db. If the same bandwidth is used for both systems only $\frac{5}{16}$ as much information is carried by system 5. However, now only a vlaue of $\beta^2 = 3.4$ db is required. Thus a decrease in transmitted power of 6 db (4 to 1) can be offset by a reduction of information rate in the ratio of 16 to 5 while maintaining the same probability of error.

As a result of these two illustrations it is apparent that some opportunity for flexibility does exist. However, Figure 17 shows that as the value of β is increased, the efficiency of the channel as given by C_x/C_{SH} decreases steadily. Therefore, to extend the work begun here it is logical to work in terms of a larger number of phase positions. For example, instead of the binary case considered here where only sample point phases of $\pm \frac{\pi}{2}$ radians are allowed, the possibility of four phase positions (0, $\pm\frac{\pi}{2}$, and π radians) at the sample points could be considered. Such a system would undoubtedly be more efficient at larger values of β. However, it is also clear that an entire continuum in number of phase positions is needed in order to be able to design a good system for any particular range of β. Efficient codes for this purpose apparently still await discovery, however.

Figures 17 and 18 do not show plotted values of channel efficiency for low values of β. These curves were arbitrarily discontinued at points corresponding to $P_E^{(n)}[\beta]$ of .8. For values lower than .8 the transition probability to the code symbol opposite from the one actually transmitted probably becomes quite important. No computer evaluations were made in this regard because of the relative importance of operation under such conditions.

Figure 4 shows the channel capacity of a phase modulation system in terms of the familiar Shannon capacity. This curve shows that in the range of values of β^2 near 0 db very efficient phase modulation communication systems are possible. The Blachman asymptote for low values of β was confirmed by the computer evaluation of Equation 17. The asymptote predicted for high values of β also appears to be correct. The approach to the asymptote was much slower than anticipated intuitively.

Over a limited range of β, this system is quite efficient in terms of Shannon's channel capacity as shown by Figure 17. However, many situations arise in which error rate, not channel efficiency, are most desirable. In such cases, reference must be made to Figure 16 for comparison of this system with others.

One undesirable characteristic of the binary phase modulation system proposed is the power handling capacity required by the output stage of the encoder. Figure 14 shows that approximately twice sample point amplitude should not seriously overload the encoder power amplifier. Conventional phase modulation systems do not have this problem since their output envelopes do not vary with time. The difficulty which arises in this binary system is basically due to the algebraic addition of the contributions of the 10 sampling functions which govern the envelope amplitude at any given instant. If, instead, more phase positions at the sample points were used, the combination of contributions would be done on the basis of vectorial addition and thus much less likely to produce high envelope peaks.

The initial goal of confining the output spectrum of the decoder has been substantially accomplished. The impulse response required by Equation

21 may be difficult to synthesize. However, it does appear that the spectrum conservation resulting in such an approach might make some effort in this regard worthwhile.

Another goal which this system was intended to achieve was simple decoder synchronization. Figure 5 shows no provision for this problem since it is expected to be a relatively minor problem. Use could be made of the 2^n cross-correlators already required by the decoder. Several synchronizing systems which depend upon the autocorrelation function being maximum with zero displacement would use these cross-correlators to adjust the frequency and phase of a stable oscillator at the decoder to properly operate the decoder decision device. In contrast, cross-correlation performed on the incoming waveform y (t) would be quite cumbersome since at least 2^{n-1} phase modulators resembling the encoder would be necessary to check the cross correlation with all possible input sequences.

The extent to which the mathematical model proposed in this paper approaches what is physically realizable remains to be determined. It appears possible to construct relatively simple devices to meet all system requirements, however.

VII. LITERATURE CITED

1. Shannon, Claude E. The mathematical theory of communication. Bell System Technical Journal 27: 379-423. 1948; 27: 623-656. 1948.

2. Woodward, P. M. Probability and information theory, with applications to radar. New York, N. Y., McGraw-Hill Book Co., Inc. 1953.

3. Fano, R. M. Communication in the presence of additive gaussian Noise. In Jackson, Willis, ed. Communication theory. pp. 169-182. New York, N. Y., Academic Press, Inc. 1953.

4. Sanders, R. W. Communication efficiency comparison of several communication systems. Proceedings of the Institute of Radio Engineers 48: 575-588. 1960.

5. Blachman, Nelson M. A comparison of the informational capacities of amplitude -- and phase -- modulation communication systems. Proceedings of the Institute of Radio Engineers 41: 748-759. 1953.

6. Bennett, W. R. Methods of solving noise problems. Proceedings of the Institute of Radio Engineers 44: 609-638. 1956.

7. Turin, George L. An introduction to matched filters. Institute of Radio Engineers Transactions on Information Theory IT-6: 317-329. 1960.

8. Peterson, W. W. Error correcting codes. New York, N. Y., John Wiley and Sons, Inc. 1961.

9. Paley, R. E. A. C. On orthogonal matrices. Journal of Mathematics and Physics 12: 311-320. 1933.

10. Leo, Y. W. Statistical theory of communication. New York, N. Y., John Wiley and Sons, Inc. 1960.

11. National Bureau of Standards. Tables of sine, cosine and exponential integrals. Washington, D. C., Author. 1940.

12. Goldman, Stanford. Information theory. New York, N. Y., Prentice-Hall, Inc. 1953.

13. Rice, S. O. Mathematical analysis of random noise. Bell System Technical Journal 23: 282-332. 1944; 24: 46-156. 1945.

VIII. SYMBOL DEFINITIONS

The mathematical symbol listing given below is not complete. It does, however, tabulate the principal ones used.

A	Sample point envelope amplitude of signal function. Defined by Equation 10.
C_{PM}	Capacity of phase modulated channel. Given by Equation 17.
C_{SH}	Capacity of communication channel using Shannon's conditions. Given by Equation 1.
C_x	Information rate for proposed phase modulation system. Given by Equation 52.
$F_1(j\omega)$	Complex transfer function of linear filter used in proposed communication system. See Equation 30.
$f_1(t)$	Impulse response of linear filter used in proposed communication system. Defined by Equation 21.
$\overline{H}_k$	A k x k Hadamard matrix. See Equation 20 and Figure 6.
$H(\lambda)$	Entropy of variable λ. Defined by Equation 2.
n	Number of bits required to select one code symbol at the encoder.
N_k	Envelope amplitude at the kth sample point in the noise waveform $\alpha(t)$. Defined by Equation 11.
$p_o[\lambda]$	Probability density function of random variable λ. Defined by Equation 12.
$p_1[\varphi\|\lambda]$	Conditional probability density function of variable λ given φ. Defined by Equation 13.
$P_C^{(n)}[\beta]$	Probability of correct decoding of code symbol carrying n bits with signal-to-noise ratio β^2. Defined by Equation 49.

$P_j^{(n)}[x_j;\beta]$	Probability density function at output of jth correlator. The code symbol carries n bits and the signal-to-noise ratio is β^2. See Equations 46, 47, and 48.
$R(\tau)$	Autocorrelation function of $s_1(t)$. Defined by Equation 24.
$s_1(t)$	Impulse train waveform entering linear filter of encoder. See Figure 9.
$S_2(j\omega)$	Complex spectrum at the output of the encoder. See Figure 13.
$s_2(t)$	Time domain waveform at the output of the encoder. See Equation 10.
$s_3(t)$	Time domain waveform at the output of the phase detector of the decoder.
t	Time in seconds.
$u_o(t)$	Unit impulse function having infinite positive pulse with zero width and unit area occurring at $t = 0$.
$u_1(t)$	Unit step function having unit magnitude for all $t > 0$ and zero magnitude for all $t < 0$.
x_1	Output signal of decoding integrator output terminals corresponding to code symbol actually sent by encoder.
x_2	Output signal of decoding integrator output terminals corresponding to opposite of code symbol actually sent by encoder.
$x_3 \cdots x_{2^n}$	Output signal of decoding integrator output terminals corresponding to code symbols orthogonal to the one actually sent by the encoder.
W	Bandwidth of narrowband waveforms in cycles per second.
$y(t)$	Time domain waveform entering decoder. Defined by Equation 19.
$\alpha(t)$	Time domain representation of noise waveform. See Equation 11.

β^2	Sample point signal-to-noise power ratio. See Equation 14.
λ	Phase of encoder output.
μ	Time interval between unit impulses in $s_1(t)$. See Figure 9.
σ^2	$2\sigma^2$ is mean square value of N_k.
φ	Phase of narrowband waveform y(t) at decoder input.
ω_o	Mean angular frequency of the band W cycles per second wide occupied by narrowband waveforms.

IX. ACKNOWLEDGEMENTS

A portion of the work described in this paper was done under the sponsorship of Collins Radio Company, Cedar Rapids, Iowa. Drs. R. L. Mc Creary and P. H. Rogers provided able supervision and guidance during this time.

The encouragement and patient counsel of Dr. R. G. Brown throughout the entire effort is especially appreciated.

X. APPENDIX A

This appendix develops the probability density function of the resultant phase due to the linear addition of a sine wave and narrowband, gaussian, white noise. This development follows closely that of Bennett (6).

Let $\alpha(t)$ be a representative wave of narrowband noise centered at radian frequency ω_o.

$$\alpha(t) = a(t) \cos \omega_o t - b(t) \sin \omega_o t \qquad A1$$

The functions a(t) and b(t) are functions of time varying slowly relative to oscillations at radian frequency ω_o. A cosine wave $A\cos\omega_o t$ is added to $\alpha(t)$. The envelope function e(t) is therefore given by

$$e(t) = \sqrt{[a(t) + A]^2 + b^2(t)}. \qquad A2$$

The phase function is designated by

$$\varphi(t) = \tan^{-1} \frac{b(t)}{a(t) + A}. \qquad A3$$

Consequently, expressions representing the sum of the cosine and noise waves can be written in the forms shown in Equation A4.

$$\begin{aligned} A\cos\omega_o t + \alpha(t) &= e(t)\cos[\omega_o t + \varphi(t)] \\ &= e(t)\left[\frac{a(t) + A}{e(t)} \cos\omega_o t - \frac{b(t)}{e(t)} \sin\omega_o t\right] \\ &= e(t)[\cos\varphi\cos\omega_o(t) - \sin\varphi\sin\omega_o t] \\ &= e(t)\cos(\omega_o t + \varphi) \end{aligned} \qquad A4$$

It is shown by Rice (13) that a(t) and b(t) are independent gaussian random variables. However, the proof of this fact is too lengthy to include here. Because a(t) and b(t) are independent gaussian variables,

their joint probability density function may be written as

$$p_2[a(t),b(t)] = \frac{1}{2\pi\sigma^2} \exp \frac{-a^2-b^2}{2\sigma^2} . \qquad A5$$

In order to change this probability density function to the (φ,e) coordinate system the respective two dimensional integrals must both be equal to unity. This is properly accomplished by letting

$$dadb = ededφ. \qquad A6$$

Change of variables to e and φ therefore leads to

$$p_3[e(t),\varphi(t)] = \frac{e(t)}{2\pi\sigma^2} \exp - \frac{e^2+A^2-2Aecos\varphi}{2\sigma^2} . \qquad A7$$

Equation A7 gives the joint probability density function of the narrowband noise and cosine wave in terms of the envelope function e(t) and the phase function $\varphi(t)$. In order to obtain the probability density function of the phase $\varphi(t)$ an integration over the possible range of the envelope function is made.

$$p_1[\varphi] = \int_0^\infty p_3[e(t), \varphi(t)]de$$

$$= \frac{1}{2\pi\sigma^2} \int_0^\infty \exp - \frac{e^2 + A^2 - 2Aecos\varphi}{2\sigma^2} ede \qquad A8$$

The integral shown in Equation A8 may be evaluated by completing the square in the exponent. The resulting expression is

$$p_1[\varphi] = \frac{\exp(-\beta^2)}{2\pi} + \frac{\beta cos\varphi}{\sqrt{\pi}} \exp(-\beta^2 sin^2\varphi) \frac{1}{\sqrt{2\pi}} \int_{-\infty}^{\sqrt{2}\beta cos\varphi} \exp - \frac{t^2}{2} dt . \qquad A9$$

$$-\pi \leq \varphi \leq \pi.$$

In Equation A9

$$\beta^2 = \frac{A^2}{2\sigma^2}. \qquad \text{A10}$$

Equation A9 is based upon the wave $A\cos\omega_o t$ having zero phase. If, instead, it had a phase angle λ the conditional probability density function is expressed as

$$p_1[\varphi|\lambda] = \frac{\exp(-\beta^2)}{2\pi} + \frac{\beta\cos(\varphi-\lambda)}{\sqrt{\pi}} \exp[-\beta^2\sin^2(\varphi-\lambda)]$$

$$\frac{1}{\sqrt{2\pi}} \int_{-\infty}^{\sqrt{2}\beta\cos(\varphi-\lambda)} \exp - \frac{t^2}{2}\, dt = p_1[\lambda|\varphi]. \qquad \text{A11}$$

$$-\pi \leq \varphi \leq \pi.$$

XI. APPENDIX B

This appendix is a brief summary of the theory of uniform sampling for narrowband waveforms. As in Appendix A, slowly varying envelope and phase functions are assumed. A real narrowband signal $s_r(t)$ is centered in a narrow band having a bandwidth of $2\pi W$ radians per second and center frequency ω_o radians per second.

$$s_r(t) = A(t)\cos[\omega_o t + \lambda(t)] \qquad \text{B1}$$

At this point it is desired to obtain a Fourier series expansion of the complex spectrum $S_r(j\omega)$ related to $s_r(t)$. However, this is not easily done since the positive and negative frequency bands are not adjacent as would be the case if the frequency band began at zero frequency. To circumvent this difficulty, a complex signal $s_c(t)$ is defined.

$$s_c(t) = s_r(t) - js_i(t) \qquad \text{B2}$$

The real part of $s_c(t)$ is $s_r(t)$. The imaginary part, however, is chosen in just such a way that the negative frequency band of $s_c(t)$ disappears (12).

Fourier transform pairs will be used for determining the complex spectrum. The various time functions are assumed to satisfy the Dirichlet

$$s_r(t) = \frac{1}{2\pi}\int_{-\infty}^{\infty} S_r(j\omega)\exp(j\omega t)d\omega$$

$$S_r(j\omega) = \int_{-\infty}^{\infty} s_r(t)\exp(-j\omega t)dt \qquad \text{B3}$$

conditions in order to make them transformable.

The Fourier transform of Equation B2 is

$$S_c(j\omega) = S_r(j\omega) - jS_i(j\omega). \qquad B4$$

In order to eliminate the negative frequency band it is necessary that

$$\begin{aligned} S_i(j\omega) &= jS_r(j\omega), \ \omega > 0 \\ &= -jS_r(j\omega), \ \omega < 0. \end{aligned} \qquad B5$$

$S_c(j\omega)$ may now be expanded in a Fourier series in the angular frequency range $\omega_o - \pi W \leq \omega \leq \omega_o + \pi W$. In Equation B6 the negative sign

$$S_c(j\omega) = \sum_{k=-\infty}^{\infty} c_k \exp\left[-j\frac{k\omega}{W}\right] \qquad B6$$

which has been included in the exponent for later convenience can be accounted for by proper adjustment of the usual definition of c_k. The last

$$c_k = \int_{\omega_o-\pi W}^{\omega_o+\pi W} \frac{1}{2\pi W} S_c(j\omega)\exp\left[j\frac{k\omega}{W}\right]d\omega = s_c\left(\frac{k}{W}\right)\frac{1}{W} \qquad B7$$

equality of Equation B7 is obtained by means of Equation B3. The complex time function $s_c(t)$ may therefore be expressed by

$$s_c(t) = \frac{1}{2\pi W}\int_{\omega_o-\pi W}^{\omega_o+\pi W}\left\{\sum_{k=-\infty}^{\infty} s_c\left(\frac{k}{W}\right)\exp\left[-j\frac{k\omega}{W}\right]\right\}\exp(j\omega t)d\omega \qquad B8$$

Goldman (12) shows by several successive manipulations that Equation B9 is a consequence of Equation B8.

$$s_r(t) = A_k \sum_{k=-\infty}^{\infty} \frac{\sin\left[\pi W(t-\frac{k}{W})\right]\cos\left[\omega_o(t-\frac{k}{W}) - \lambda_k\right]}{\pi W(t-\frac{k}{W})} \qquad B9$$

Equation B9 demonstrates that a narrowband signal is completely

specified by two numbers (A_k and λ_k) at the kth sample point. Sample points are regularly spaced by $\frac{1}{W}$ seconds. A_k determines the magnitude of the $\frac{\sin x}{x}$ envelope function centered at the kth sample point. The envelope function is equal to zero at all other sample points. The value of λ_k determines the carrier phase at the kth sample point.